Mechanical Engineering Advances 2025, 3(3), 2529.
https://doi.org/10.59400/mea2529

Article

Multi-objective Thermal Exchange Optimization algorithm applied to mechanical system design

Fran S. Lobato[1,*], Fabian A. Lara-Molina[2]

[1] School of Chemical Engineering, Federal University of Uberlândia, Uberlândia 38408-100, Brazil

[2] Department of Mechanical Engineering, Federal University of Triângulo Mineiro, Uberaba 38025-180, Brazil

*** Corresponding author:** Fran S. Lobato, fslobato@ufu.br

CITATION

Lobato FS, Lara-Molina FA. Multi-objective Thermal Exchange Optimization algorithm applied to mechanical system design. Mechanical Engineering Advances. 2025; 3(3): 2529. https://doi.org/10.59400/mea2529

ARTICLE INFO

Received: 8 January 2025
Revised: 20 May 2025
Accepted: 26 May 2025
Available online: 2 July 2025

Abstract: Engineering system design is a highly relevant and dynamic field, with numerous applications reported in the literature. This type of problem generally encompasses several objectives and constraints, including those arising from mass, energy, and momentum balances, material behavior equations, and a range of environmental, physical, and operational restrictions. To address such challenges, a range of evolutionary optimization strategies has been proposed and evaluated. This work presents a Multi-objective Thermal Exchange Optimization (MTEO) algorithm that integrates concepts of Pareto dominance along with crowding distance strategies. To assess its performance, the proposed algorithm is applied to three well-established mechanical design problems. The results demonstrate that the MTEO algorithm provides accurate approximations of the Pareto front in comparison with conventional evolutionary methods. Specifically, average reductions of approximately 36%, 32%, and 68% were observed for the respective design problems. Furthermore, the MTEO parameters were found to be easy to configure across all applications.

Keywords: multi-objective optimization; Thermal Exchange Optimization; engineering system design; mechanical problem

1. Introduction

The concept of design problems in engineering dates back to the early Industrial Revolution, a period marked by a significant demand for more sophisticated and efficient solutions to technical, mechanical, and structural challenges [1,2]. Over time, this concept has evolved, becoming formalized within engineering and architectural disciplines, particularly with the advancement of interdisciplinary design practices and the introduction of user-centered design in the latter part of the 20th century [1]. The systematic treatment of engineering design problems began in the early 20th century but gained considerable momentum from the 1960s onward [2]. It is important to emphasize the complexity (non-linearity) of the models that represent the constraints in a design problem. In this context, highly complicated patterns can be found across various research fields [3–6].

In recent decades, numerous algorithms for both mono-objective and multi-objective engineering system design have been proposed, driven by the nonlinearities inherent in mass, energy, and momentum balances [7]. Optimization problems of this nature may be addressed through deterministic or non-deterministic techniques. Deterministic methods utilize predefined information about the objective function and constraints to progressively improve potential solutions. Notable

deterministic methods include the Interior Point Method, Newton's Method, and Sequential Quadratic Programming [8]. These methods have the advantage of converging to an optimal solution with relatively few iterations. Nevertheless, these methods face difficulties when dealing with discontinuities and multi-modal objective functions. They are generally unsuitable for multi-objective optimization since they are unable to capture the full Pareto front in one execution. Furthermore, approaches based on derivatives often converge to local optima [9].

In comparison, non-deterministic methods operate without the need for precise information about the objective function or its constraints. Instead, they rely on a population of candidate solutions that evolve over successive iterations, guided by heuristics inspired by natural phenomena such as biological, physical, or chemical processes [10]. One major drawback of these methods is their high computational cost, as they require numerous evaluations of the objective function due to the population-based approach. One of the pioneering and most impactful population-based techniques in this field was the Genetic Algorithm [11]. Following its development, numerous other approaches have emerged, such as Differential Evolution [12] and Particle Swarm Optimization [13].

The study of engineering systems design problems is essential because it enables the identification and analysis of the needs and limitations of the system or product to be developed. Engineers can seek more efficient, safe, and sustainable solutions in this process, minimizing risks and optimizing resources. Moreover, it is important to highlight that solving the design problem facilitates decision-making, ensuring that technical choices meet the requirements of the case study while adhering to deadlines and budgets. This problem inherently involves the optimization of multiple interconnected objectives, such as performance, cost, durability, and environmental impact. As a result, a trade-off solution must be found between these often conflicting objectives. In mechanical systems design, various contributions can be found in the specialized literature. Notable examples include reliability-based design of high-performance hydrocyclones [14], breast cancer treatment using hyperthermia [15], mechanical systems design [16, 17], and design of robotic manipulators considering uncertainties [18, 19].

In general terms, population-based methods have been used for the design of engineering systems. This is due, among other factors, to the global search capability of these algorithms [12]. A more recent approach is the Thermal Exchange Optimization (TEO) algorithm, introduced by Kaveh and Dadras [20], initially developed to address single-objective mathematical functions and mechanical design benchmarks. The TEO algorithm generates candidate solutions based on Newton's law of cooling, simulating the optimization process as a thermal exchange system. TEO has since been applied across various scientific and engineering fields, including structural optimization [21, 22], energy management [23], tuning proportional-integral controllers for doubly-fed induction generators in wind energy applications [24], smart healthcare systems [25], network intrusion detection [26], and vehicular ad-hoc networks [27]. More recently, Kumar et al. [28] extended the TEO method to address multi-objective optimization in truss structure design.

Studies published in the specialized literature indicate that these algorithms effectively provide good approximations for finding optimal solutions. As highlighted by Wolpert and Macready [29], no single optimization technique is universally effective for all problem types. This realization drives ongoing efforts within the scientific community to refine existing methods or design novel algorithms, especially in response to new challenges emerging from scientific progress. It is also important to note that a considerable amount of new metaheuristic algorithms have been introduced in recent years, making it essential to validate and compare their performance against well-established techniques. These comparisons are crucial, even to determine whether a particular algorithm applies to a specific class of problems. In this regard, a robust stochastic optimization algorithm should possess several key features [30]: (i) exploration (or diversification) to ensure broad coverage of the search space; (ii) exploitation (or intensification) to effectively refine solutions near potential global optima; (iii) convergence, representing the clustering of solutions around the optimum; (iv) the ability to avoid premature convergence; and (v) a fast convergence rate. As a result, engineering applications offer an appropriate and challenging environment for evaluating the performance of such algorithms [31]. Additionally, transitioning from single-objective algorithm to the multi-objective framework is more than just a modification of the problem's dimensions. However, it requires a fundamental shift in how the methodology is evaluated. Finally, as noted by Sorensen [32], enhancing the performance of existing metaheuristics by incorporating specific operators may, in some cases, be more beneficial than developing entirely new algorithms [33].

The present work proposes the Multi-objective Thermal Exchange Optimization (MTEO) algorithm to address problems involving multiple objectives. The method integrates the original TEO framework with two key mechanisms: Pareto dominance and crowding distance. To analyze the capability of the proposed strategy, three case studies from the field of mechanical engineering are examined. The novelty of this research lies not only in creating a multi-objective optimization algorithm with TEO method combined with two essential operators—crowding distance and Pareto dominance—as well as within the formulation and evaluation of several case studies centered on mechanical process design. It should be noted that the individual application of each operator was not proposed in the present work.

This manuscript is structured in the following manner: Section 2 presents some population-based optimization strategies within the scope of multi-objective optimization. A comprehensive review of the Thermal Exchange Optimization (TEO) algorithm is provided in Section 3. Fundamental principles of multi-objective optimization are covered in Section 4. Then, Section 5 details how TEO algorithm is extended to handle multi-objective problems. Section 6 provides an evaluation and discussion of outcomes from three case studies. Lastly, the key findings are summarized in Section 7.

2. Population-based optimization algorithms for solving multi-objective problems

The design problem typically involves optimizing multiple conflicting objectives simultaneously. Typically, numerical techniques designed for addressing multi-objective optimization challenges rely on population-based algorithms. Population-based algorithms are often chosen because of their capability to avoid falling into local optima [12]. The earliest definition of a numerical method for this context was provided by Schaffer [34] through the concept of Pareto dominance [35]. Since that time, numerous algorithms have been introduced to address multi-objective optimization problems. Among the most prominent multi-objective evolutionary algorithms is the Multi-objective Optimization Vibrating Particle System (MOVPS) [7], which combines the operators from the original VPS method with the Pareto dominance principle and a mutation operator; The Multi-objective Optimization Shuffled Complex Evolution with Local Search (MOSCE-LS) algorithm [17] incorporates Shuffled Complex Evolution (SCE) operators alongside the Pareto dominance principle to guide the search process; Non-dominated Sorting Genetic Algorithm (NSGA-II) [36] (within this classical optimization method, the association between GA operators, crowding distance, and the Pareto dominance criterion is established); Multi-objective Optimization Differential Evolution (MODE) algorithm [37] integrates Differential Evolution (DE) operators with crowding distance, the Pareto dominance strategy, and a neighborhood generation mechanism to enhance search performance; Multi-Objective Water Cycle Algorithm [38] (in this optimization algorithm, the association between the Water Cycle Algorithm operators, crowding distance, and the Pareto dominance criterion is established); Multi-Objective Grey Wolf Optimizer [39] (this strategy consists of the association between the Grey Wolf Algorithm operators, crowding distance, and the Pareto dominance criterion); Multi-Objective Ant Lion Optimizer [40] (the Ant Lion Optimizer operators are associated with the crowding distance strategy and the Pareto dominance criterion); Multi-Objective Particle Swarm Optimization (MOPSO) [41] (in this optimization algorithm, the Particle Swarm Optimization strategy is combined with the crowding distance strategy, the Pareto dominance criterion, and a mutation operator); Multi-Objective Optimization Stochastic Fractal Search (MOPSO) [42] (the Stochastic Fractal Search algorithm is associated with the crowding distance strategy and the Pareto dominance criterion) and Multi-Objective Optimization Flower Pollination (MOFP) [43] (the Flower Pollination strategy is combined with the crowding distance strategy and the Pareto dominance criterion).

3. Thermal Exchange Optimization

As noted earlier, the Thermal Exchange Optimization (TEO) algorithm draws inspiration from Newton's law of cooling, which describes how the rate of heat loss from an object is proportional to the temperature difference between the object and its environment [20]. Within this framework, In the TEO algorithm, each particle is represented as an object undergoing either heating or cooling processes. By associating

each particle with an environmental agent, thermal exchange and heat transfer occur between them. Following the application of specific operators aimed at enhancing the current population, the updated temperature of the object—corresponding to the design variables—defines its subsequent position in the search space. The following section offers a brief summary of the TEO algorithm.

3.1. Mathematical description

The steps outlined below are considered when applying the method to solve the mono-objective optimization problem.

3.1.1. Initialization, evaluation and memory

Like other population-based metaheuristics, TEO is initialized by considering a group of randomly produced temperatures (candidate solutions to the optimization problem). For this purpose, the following relation is used:

$$T_j^i = T_{j,\text{min}}^i + r(T_{j,\text{max}}^i - T_{j,\text{min}}^i) \tag{1}$$

where T_j^i is the initial temperature of the i-th potential solution related to j-th design variable, $T_{j,\text{min}}^i$ and $T_{j,\text{max}}^i$ represent the minimum and maximum limits for each design variable, and r is randomly generated value uniformly distributed within [0 1]. In this case, a set of N temperatures (population size) is generated.

Each potential candidate is evaluated considering the objective function (which defines the optimization problem). The top-performing solutions, with respect to the objective function, are saved throughout the evolutionary mechanism. To enhance the efficiency of the TEO method, these best solutions are incorporated into the current population, and an equal number of the least-performing candidates are eliminated. Finally, the potential candidates are ranked based on their corresponding objective function sorted from lowest to highest.

3.1.2. Creating groups

In the TEO algorithm, the potential candidates are sorted from lowest to highest with respect to the objective function (the best candidate is the hottest and the worst candidate is the coldest). The current population is organized into two groups with an equal number of candidates. Thus, considering N candidates, each subset consists of the first half ($i = 1, \ldots, N/2$) and the second half ($i = N/2 + 1, \ldots, N$). In this situation, the first half contains the warmest candidates, and the second half contains the coldest candidates.

3.1.3. Updating the current population

Derived from Newton's Law of Cooling, each candidate is updated ($T_{j,\text{new}}^i$) considering the following relation:

$$T_{j,\text{new}}^i = T_{j,\text{env}}^i + \exp(-\gamma_i t)(T_j^i - T_{j,\text{env}}^i) \tag{2}$$

$$T_{j,\text{env}}^i = (1 - (c_1 + c_2(1-t)) \times r)T_j^i \tag{3}$$

where $T^i_{j,env}$ corresponds to the new position of the cooled or heated individual, r represents a randomly generated value uniformly distributed within [0 1], c_1 and c_2 are the controlling parameters chosen from 0 or 1. (1-t) decreases the randomness linearly and progressively intensifies exploitation toward the later iterations. As mentioned by Kaveh and Dadras [20], any potential candidate will be either regenerated, updated, cooled, or heated.

The control parameters t and γ_i can be updated as:

$$t = \frac{NI}{NI_{\text{max}}} \tag{4}$$

$$\gamma_i = \frac{OF_i}{OF_{\text{max}}} \tag{5}$$

where NI and NI_{max} are the present generation count of the algorithm and the highest number of algorithm generations (the stopping criterion considered), respectively. OF_i and OF_{max} represent the definition of the i-th objective function and the worst value of the current population (the coldest candidate), respectively.

It is worth noting that updating the potential candidates according to Equation (2) may allow escape from a local optimum. γ increases in direct relation to the penalized objective function of each potential candidate, i.e., the best solution will be set to the lowest value of γ, and the worst or coldest object will be assigned a value of 1. Additionally, at the end of the evolutionary algorithm, if t increases, this leads to a gradual linear reduction in randomness and an increase in exploitation [20].

To improve the chances of the TEO algorithm escaping from a local optimum, an additional parameter, ρ, within the interval (0,1), is considered. For each potential candidate, ρ is compared with r_j ($j = 1, 2, \ldots, N_D$, where N_D is the number of design variables), which is a uniformly distributed random variable within (0,1). If $r_j < \rho$, one dimension of the j-th design variable is chosen at random, then its value is recalculated as follows:

$$T^i_j = T^i_{j,\text{min}} + r(T^i_{j,\text{max}} - T^i_{j,\text{min}}) \tag{6}$$

where T^i_j is the j-th variable of the i-th potential candidate, and $T^i_{j,\text{min}}$ and $T^i_{j,\text{max}}$ are the minimum and maximum limits of the j-th design variable, respectively. As mentioned by Kaveh and Dadras [20], this simple mechanism enhances the diversity within the current population. As a consequence, convergence to a local solution can be avoided.

3.1.4. Stopping criterion

As mentioned earlier, the greatest number of generations is employed as a stopping rule.

4. Multi-objective optimization

The mathematical definition of the problem involving multiple objectives is given by [10]:

$$\begin{aligned} &\min \mathbf{f}(\mathbf{x}) \\ &\text{Subject to } \mathbf{g}(\mathbf{x}) \leq \mathbf{0} \\ &\mathbf{h}(\mathbf{x}) = \mathbf{0} \\ &\mathbf{x}^{\text{inf}} \leq \mathbf{x} \leq \mathbf{x}^{\text{sup}} \end{aligned} \tag{7}$$

$\mathbf{x}$ corresponds to the design variables vector, confined to $\mathbf{x}^{\text{inf}}$ and $\mathbf{x}^{\text{sup}}$, $\mathbf{f}$ is defined as the vector of multi-objective, $\mathbf{g}$ denotes the inequality constraints, while $\mathbf{h}$ denotes the equality constraints.

Unlike the mono-objective problem, where the definition of the optimal solution is well established, multi-objective problems do not have a formal definition. Instead, a concept is used to characterize the optimal solution, known as Pareto dominance or simply the Pareto curve [35]. The optimal solution is composed of a collection of non-dominated solutions that outline the Pareto front. This approach provides a method for comparing potential solutions that belong to this front in multi-objective optimization problems. In this context, a feasible solution $\mathbf{x}^1$ is said to *dominate* another solution $\mathbf{x}^2$, expressed as $\mathbf{x}^1 \prec \mathbf{x}^2$, if both of the conditions below are satisfied [10]: i) solution $\mathbf{x}^1$ is no worse than $\mathbf{x}^2$ in all objectives, that is, $f_k\left(\mathbf{x}^1\right) \leq f_k\left(\mathbf{x}^2\right)$, for all $k = 1, \ldots, m$; i) solution $\mathbf{x}^1$ is strictly better than $\mathbf{x}^2$ in at least one objective, that is, $f_k\left(\mathbf{x}^1\right) < f_k\left(\mathbf{x}^2\right)$ for some $k \in \{1, \ldots, m\}$.

Thus, a solution is considered dominant over another if it performs at least as well in all objectives and if it shows improvement with respect to at least one objective function. If one or more of these conditions are not satisfied, solution $\mathbf{x}^1$ is considered not to dominate solution $\mathbf{x}^2$.

5. Multi-objective Thermal Exchange Optimization

Figure 1 presents the main operators of the Multi-objective Thermal Exchange Optimization (MTEO) algorithm, which are briefly described below.

Initially, a population of N individuals is randomly generated. Every dominated solution is excluded from the population using the Pareto dominance operator (see Section 4). The remaining individuals are subsequently organized into non-dominated fronts F_j, where each front comprises mutually non-dominated solution vectors. This procedure continues iteratively until all vectors have been allocated to a corresponding front. Next, potential candidates are generated using the TEO operators (see Section 3) until N new candidates have been produced. The updated population is then evaluated and ranked in accordance with the dominance criterion. If the number of individuals exceeds a user-defined threshold, the population is truncated based on the crowding distance criterion [10]. Mathematically, the aforementioned operator is represented by the following relation:

$$dist_{x_i} = \sum_{j=0}^{M-1} \frac{f_{j,i+1} - f_{j,i-1}}{|f_{j,\max} - f_{j,\min}|} \tag{8}$$

where $dist_{x_i}$ denotes the spacing between the two nearest neighbors with respect to the candidate solution x_i, f_j corresponds to the j-th objective function ($f_{j,\min}$ and $f_{j,\max}$) represent the lower and upper bounds for the j-th objective function) where M denotes the number of objective functions.

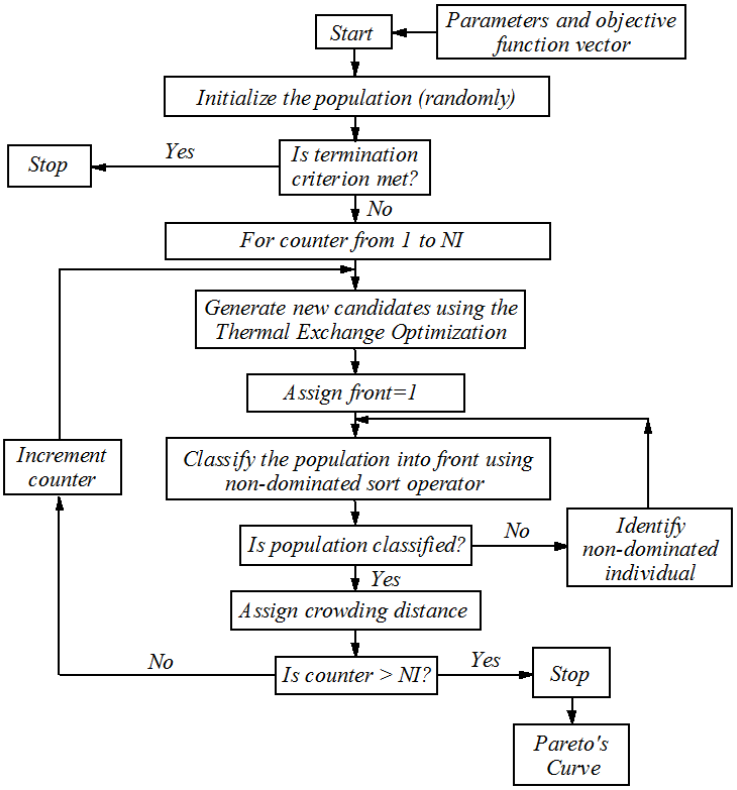

Figure 1. MTEO algorithm flowchart.

Regarding the strategy developed by Khodadadi et al. [44], which also relies on the TEO algorithm to generate potential candidates, the proposed methodology is similar — both use the Pareto dominance criterion and the crowding distance operator. However, they differ in how the control parameter t is computed, as well as in the manner in which dominated individuals are eliminated from the current population. In the strategy proposed by Khodadadi et al. [44], points with higher ranks are eliminated, whereas in the algorithm proposed in this work, dominated points are discarded based on the rank analysis and the distance computed by the crowding distance operator.

6. Results and analysis

6.1. Mathematical functions

The classical ZDT functions [45] are considered to validate the proposed methodology's performance. To achieve this, the subsequent multi-objective optimization strategies are applied: Non-dominated Sorting Genetic Algorithm (NSGA-II) [36] (the population size is set to 105, with a crossover probability of 0.85 and a mutation probability of 0.05. The selection strategy employed is binary

tournament); Multi-objective Optimization Differential Evolution (MODE) [37] (Population size—105, crossover probability—0.85, perturbation rate—0.5, and Strategy 7 is adopted in the optimization process (see [12])); Multi-Objective Particle Swarm Optimization Optimization (MOPSO) [41] (Population size—105, initial acceleration factor—2.5, final acceleration factor—0.5, initial inertia factor—0.9, and final inertia factor—0.4); Multi-Objective Evolutionary Algorithm Based on Decomposition (MOEA/D) [46] (Population size—105, crossover probability—0.85, perturbation rate—0.95, neighbour update probability—0.95, as well as the number of adjacent subproblems—5); Multi-objective Optimization Shuffled Complex Evolution with Local Search (MOSCE-LS) [17] (Population size—105, number of complexes—5, and total number of sampling points—2); Multi-objective Vibrating Particles System (MOVPS)[7] (Population size—105, mutation probability—0.05, weights—0.3, 0.3, and 0.4, and parameter p—0.1); and MTEO (Population size—105, c_1—0.5, c_2—0.5, and ρ—0.3).

The area under the Pareto front is used as a convergence criterion to establish the stopping criterion for all algorithms under study. The evolutionary process is terminated when the absolute difference between the area at the current generation and the mean area of the preceding 50 generations is below 1×10^{-5}. When this requirement is not fulfilled, the algorithm persists until reaching the specified maximum number of generations (5000 in this case). To ensure statistical robustness, for each algorithm, 20 independent runs are performed using 20 distinct random seeds for population initialization.

Mathematically, the ZDT functions are defined as follows [45]):

$$\text{minimize} \ \ (f_1(x),\ f_2(x)) \tag{9}$$

where:

$$f_1(x) = x_1 \tag{10}$$

For each function, $f_2(x)$ and $G(x)$ are given as follows.

ZDT_1 (convex function):

$$f_2(x) = G(x)\left(1 - (f_1(x)/G(x))^{0.5}\right) \tag{11}$$

$$G(x) = \left(1 + 9\sum_{i=2}^{m}\frac{x_i}{m-1}\right) \tag{12}$$

ZDT_2 (non-convex function):

$$f_2(x) = G(x)\left(1 - (f_1(x)/G(x))^{2}\right) \tag{13}$$

$$G(x) = \left(1 + 9\sum_{i=2}^{m}\frac{x_i}{m-1}\right) \tag{14}$$

ZDT_3 (continuous convex function):

$$f_2(x) = G(x)\Phi \tag{15}$$

where

$$\Phi = 1 - (f_1(x)/G(x))^{0.5} - (f_1(x)/G(x))\sin(10\pi f_1(x)) \tag{16}$$

$$G(x) = \left(1 + 9\sum_{i=2}^{m}\frac{x_i}{m-1}\right) \tag{17}$$

The design space considered for these functions is constrained within the bounds $x_i \in [0,1]$ ($i = 1,\ldots,m$). In addition, the optimal result occurs at $x_1 \in [0,1]$ and $x_i = 0$ for $i = 2,\ldots,m$=10.

The following metrics are employed to assess the quality of solutions obtained by each multi-objective optimization strategy: convergence (Υ) and diversity (Δ). Mathematically, these are defined as [10]:

$$\Upsilon = \frac{\sum_{i=1}^{|Q|} d_i}{|Q|} \tag{18}$$

$$\Delta = \frac{d_f + d_l + \sum_{i=1}^{|Q|-1}|d_i - \overline{d}|}{d_f + d_l + (|Q|-1)\overline{d})} \tag{19}$$

where d_i denotes the Euclidean distance between each of the Q non-dominated solutions obtained through the evolution-based optimization method and their corresponding points on the Pareto-optimal front. The symbol $\overline{d}$ indicates the mean of these distances, whereas d_l and d_f are associated with the distances between the endmost (boundary) solutions and the Pareto-optimal solutions.

To evaluate whether or not there is a statistically significant difference between the median values (Υ and Δ) of three or more algorithms, the Kruskal-Wallis test [47] considering 5% of significance level is applied. If the null hypothesis for this test is reject, the following hypotheses are tested:

- $\mathcal{H}_0$: there is no difference between the obtained results for each pair of analyzed algorithms;
- $\mathcal{H}_1$: there is a difference between each pair of analyzed algorithms.

Table 1 compiles the comparative metrics of each multi-objective algorithm, using a reference front composed of 1000 uniformly spaced optimal solutions. The results indicate that all algorithms are capable of obtaining good approximations of the Pareto front, as evidenced by the reported average and standard deviation values.

Regarding the number of objective function evaluations (n_{eval}), the results show that the proposed algorithm achieves optimal solutions characterized by effective convergence and maintained diversity, outperforming conventional multi-objective optimization techniques across all ZDT test functions. For the ZDT_1 function, the proposed algorithm leads to percentage reductions of approximately 2.5%, 10.9%, 10.2%, 11.9%, 8.8%, and 3.9% compared to the NSGA-II, MODE, MOPSO, MOEA/D, MOSCE, and MOVPS algorithms, respectively. For the ZDT_2 function, the reductions are 4.5%, 3.6%, 0.2%, 8.5%, 7.1%, and 4.1%, respectively. Finally, for the ZDT_3 function, the reductions are 4.3%, 2.9%, 19.9%, 18.1%, 2.1%, and 6.5%, respectively, for the same algorithms.

Table 1. The mean (μ), standard deviation (σ), and the total number of objective function evaluations (n_{eval}) are presented for the algorithms NSGA-II, MODE, MOPSO, MOEA/D, MOSCE, MOVPS, and MTEO.

	ZDT$_1$		
	$\mu(\Upsilon)/\sigma(\Upsilon)$	$\mu(\Delta)/\sigma(\Delta)$	$\mu(n_{eval})/\sigma(n_{eval})$
NSGA-II	$4.26 \times 10^{-3}/1.11 \times 10^{-3}$	$1.21 \times 10^{-1}/1.96 \times 10^{-2}$	71,289/10,302
MODE	$3.44 \times 10^{-3}/8.51 \times 10^{-4}$	$1.38 \times 10^{-1}/2.18 \times 10^{-2}$	78,146/13,161
MOPSO	$7.84 \times 10^{-3}/9.87 \times 10^{-4}$	$1.57 \times 10^{-1}/2.89 \times 10^{-2}$	77,454/17,345
MOEA/D	$3.01 \times 10^{-3}/5.45 \times 10^{-4}$	$1.32 \times 10^{-2}/3.33 \times 10^{-2}$	78,985/19,858
MOSCE	$3.22 \times 10^{-3}/6.78 \times 10^{-4}$	$1.44 \times 10^{-1}/2.61 \times 10^{-2}$	76,266/8157
MOVPS	$3.25 \times 10^{-4}/2.34 \times 10^{-5}$	$1.45 \times 10^{-1}/3.45 \times 10^{-2}$	72,454/9457
MTEO	$3.45 \times 10^{-4}/1.23 \times 10^{-5}$	$1.54 \times 10^{-1}/2.54 \times 10^{-3}$	69,574/8232
	ZDT$_2$		
	$\mu(\Upsilon)/\sigma(\Upsilon)$	$\mu(\Delta)/\sigma(\Delta)$	$\mu(n_{eval})/\sigma(n_{eval})$
NSGA-II	$3.11 \times 10^{-3}/7.50 \times 10^{-4}$	$1.62 \times 10^{-1}/1.33 \times 10^{-2}$	82,010/56,073
MODE	$3.66 \times 10^{-3}/8.86 \times 10^{-4}$	$1.44 \times 10^{-1}/1.93 \times 10^{-2}$	81,280/12,606
MOPSO	$4.46 \times 10^{-3}/2.78 \times 10^{-4}$	$2.70 \times 10^{-1}/3.06 \times 10^{-2}$	78,466/12,762
MOEA/D	$3.04 \times 10^{-3}/4.53 \times 10^{-4}$	$1.81 \times 10^{-1}/2.99 \times 10^{-2}$	85,576/20,998
MOSCE	$3.12 \times 10^{-3}/6.53 \times 10^{-4}$	$1.61 \times 10^{-1}/2.19 \times 10^{-2}$	84,304/11,696
MOVPS	$2.98 \times 10^{-4}/3.98 \times 10^{-5}$	$1.66 \times 10^{-1}/2.32 \times 10^{-2}$	81,634/10,754
MTEO	$2.83 \times 10^{-4}/2.54 \times 10^{-5}$	$2.34 \times 10^{-1}/1.23 \times 10^{-3}$	78,343/8958
	ZDT$_3$		
	$\mu(\Upsilon)/\sigma(\Upsilon)$	$\mu(\Delta)/\sigma(\Delta)$	$\mu(n_{eval})/\sigma(n_{eval})$
NSGA-II	$3.74 \times 10^{-3}/9.01 \times 10^{-4}$	$3.09 \times 10^{-1}/1.59 \times 10^{-2}$	65,514/15,895
MODE	$3.69 \times 10^{-3}/1.13 \times 10^{-3}$	$3.15 \times 10^{-1}/2.24 \times 10^{-2}$	64,611/20,735
MOPSO	$3.68 \times 10^{-3}/2.84 \times 10^{-4}$	$2.78 \times 10^{-1}/3.66 \times 10^{-2}$	78,232/16,663
MOEA/D	$3.88 \times 10^{-3}/1.56 \times 10^{-3}$	$3.23 \times 10^{-1}/3.66 \times 10^{-2}$	76,454/19,498
MOSCE	$3.93 \times 10^{-3}/1.41 \times 10^{-3}$	$3.13 \times 10^{-1}/2.26 \times 10^{-2}$	64,002/17,556
MOVPS	$3.72 \times 10^{-3}/7.49 \times 10^{-6}$	$2.56 \times 10^{-1}/3.44 \times 10^{-2}$	66,996/10,878
MTEO	$4.54 \times 10^{-3}/3.81 \times 10^{-5}$	$1.98 \times 10^{-1}/6.76 \times 10^{-3}$	62,678/9254

Figures 2–4 illustrate the Pareto curves generated by the proposed algorithm alongside their analytical solutions. These results plainly reveal that the MTEO algorithm provides a highly accurate approximation of the optimal solution.

Table 2 presents the p-value considering the combination between MTEO and other evolutionary strategies. In this table, NS (Not Significant) means that, for such a pair of algorithms, there are no differences between the results of the algorithms ($\mathcal{H}_0$ was accepted). On the other hand, if the p-value is lower than the significance level (5%), the null hypothesis must be rejected.

For the convergence metric, in this table it is important to observe that there are differences between the results obtained by the proposed methodology and the approaches NSGA-II (all ZDT functions), MODE (function ZDT$_3$), MOPSO (all ZDT functions), MOED/D (functions ZDT$_2$ and ZDT$_3$), MOSCE (functions ZDT$_1$ and ZDT$_2$) and MOVPS (function ZDT$_3$). On the other hand, the null hypothesis $\mathcal{H}_0$ is accepted for the other pairs.

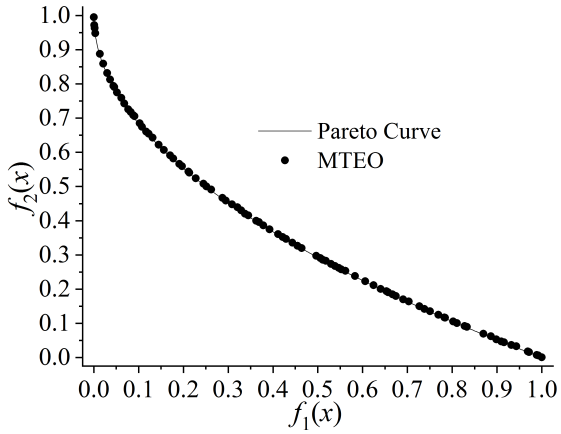

Figure 2. Pareto front for the ZDT_1 function generated by the MTEO algorithm compared to the analytical solution.

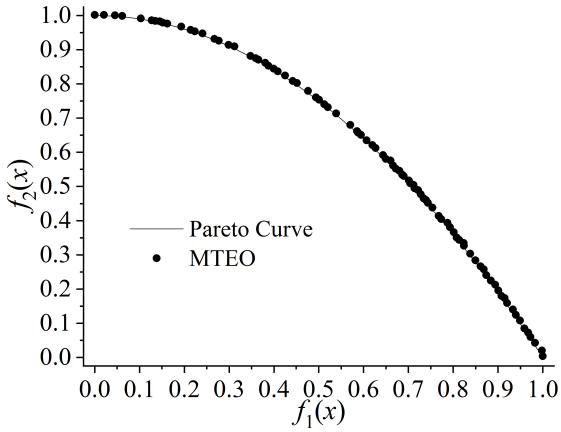

Figure 3. Pareto front for the ZDT_2 function generated by the MTEO algorithm compared to the analytical solution.

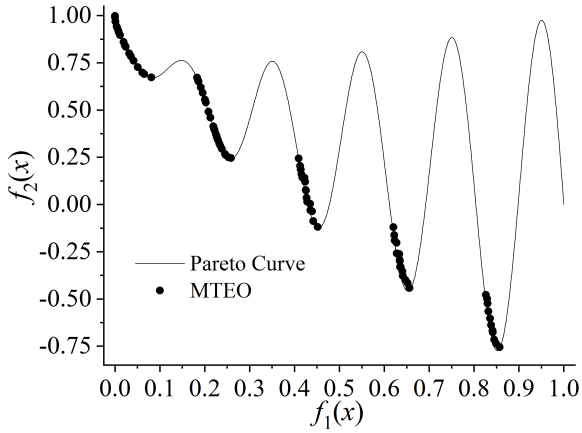

Figure 4. Pareto front for the ZDT_3 function generated by the MTEO algorithm compared to the analytical solution.

A similar analysis can be realized for the diversity metric, i.e.; there are differences between the results obtained by the MTEO approach and the strategies NSGA-II (all ZDT functions), MODE (function ZDT_3), MOPSO (functions ZDT_1 and ZDT_3), MOSCE (functions ZDT_1 and ZDT_3) and MOVPS (function ZDT_3). On the other

hand, the null hypothesis $\mathcal{H}_0$ is accepted for the other pairs.

Table 2. p-value for each combination MTEO versus NSGA-II, MODE, MOPSO, MOEA/D, MOSCE and MOVPS (NS = Not Significant).

	ZDT_1—Convergence					
	NSGA-II	MODE	MOPSO	MOEA/D	MOSCE	MOVPS
MTEO	< 0.05	**NS**	< 0.05	**NS**	< 0.05	**NS**
	ZDT_1—Diversity Metric					
	NSGA-II	MODE	MOPSO	MOEA/D	MOSCE	MOVPS
MTEO	< 0.05	**NS**	< 0.05	**NS**	< 0.05	**NS**
	ZDT_2—Convergence					
	NSGA-II	MODE	MOPSO	MOEA/D	MOSCE	MOVPS
MTEO	< 0.05	**NS**	< 0.05	< 0.05	< 0.05	**NS**
	ZDT_2—Diversity Metric					
	NSGA-II	MODE	MOPSO	MOEA/D	MOSCE	MOVPS
MTEO	< 0.05	**NS**	**NS**	**NS**	**NS**	**NS**
	ZDT_3—Convergence					
	NSGA-II	MODE	MOPSO	MOEA/D	MOSCE	MOVPS
MTEO	< 0.05	< 0.05	< 0.05	< 0.05	**NS**	< 0.05
	ZDT_3—Diversity Metric					
	NSGA-II	MODE	MOPSO	MOEA/D	MOSCE	MOVPS
MTEO	< 0.05	< 0.05	< 0.05	**NS**	< 0.05	< 0.05

In summary, considering the results presented in this table, it can be observed that the comparisons between the proposed methodology and the other strategies indicate—in most cases—significant statistical differences. However, it is important to mention that the results, for each optimization strategy, are dependent on a set of parameters. Thus, ultimately, we expect distinct results arising from different techniques, even with the same patterns for convergence and diversity metrics.

In the next sections, the MTEO algorithm is tested on three classical mechanical design problems. To compare the performance of MTEO, we evaluate the results obtained against those of other multi-objective optimization strategies. The maximum number of generations is used as the stopping rule applied to each algorithm. To assess the influence of the MTEO parameters, the area under the Pareto curve is computed. This metric is chosen because the selected design problem lacks an analytical solution, making it impossible to compute traditional convergence and diversity metrics [10]. Finally, it is important to emphasize that the MTEO algorithm was executed 20 times.

6.2. Beam design

Consider a beam with an I-cross-section studied by Castro [16], as shown in **Figure 5**. The beam is subjected to two loads: a vertical load P (600 kN) and a horizontal load Q (50 kN), both applied at the midpoint of the beam. The design variables are the dimensions x_1, x_2, x_3, and x_4, and the objective functions are given

by the cross-sectional area (cm^2) and the maximum static displacement (cm):

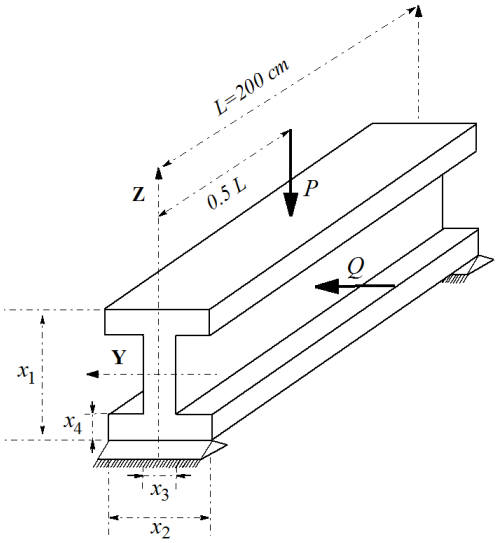

Figure 5. Schematic representation of an I-beam.

$$\min f_1 = 2x_2x_4 + x_3(x_1 - 2x_4) \tag{20}$$

$$\min f_2 = \frac{PL^3}{48EI} \tag{21}$$

where the moment of inertia I is calculated as:

$$I = \frac{x_3(x_1 - 2x_4)^3 + 2x_2x_4(4x_4^2 + 3x_1(x_1 - 2x_4))}{12} \tag{22}$$

and E is Young's Modulus (2×10^4 kN/cm^2) and σ is the beam's design stress (16 kN/cm^2). The bounds for this application are given as [16]: 10 cm $\leq x_1 \leq$ 80 cm, 10 cm $\leq x_2 \leq$ 50 cm, 0.9 cm $\leq x_3 \leq$ 5 cm, and 0.9 cm $\leq x_4 \leq$ 5 cm. Additionally, the following design constraint is considered:

$$g(x) \equiv \frac{M_{\mathbf{Y}}}{W_{\mathbf{Y}}} + \frac{M_{\mathbf{Z}}}{W_{\mathbf{Z}}} \leq \sigma \tag{23}$$

where $M_{\mathbf{Y}}$ (30,000 kN·cm) and $M_{\mathbf{Z}}$ (25,000 kN·cm) correspond to the maximum bending moments along the Y and Z axes, respectively, and $W_{\mathbf{Y}}$ and $W_{\mathbf{Z}}$ represent the section moduli in those respective directions. The resistance modules are computed as follows:

$$W_{\mathbf{Y}} = \frac{x_3(x_1 - 2x_4)^3 + 2x_2x_4(4x_4^2 + 3x_1(x_1 - 2x_4))}{6x_1} \tag{24}$$

$$W_{\mathbf{Z}} = \frac{(x_1 - 2x_4)x_3^3 + 2x_4x_2^3}{6x_2} \tag{25}$$

To find a solution for this mechanical design problem, the following MTEO parameters are taken into account: N = 50, $NI_{\max}$ = 240, $c_1 = c_2$ = 0.5, and ρ = 0.3 (these parameters represent 12,050 objective function evaluations). It is important to

note that these parameters were chosen based on prior runs to decrease the number of objective function evaluations without compromising solution quality in comparison with the results documented by other studies.

6.2.1. Pareto curve

Figure 6 presents the solutions obtained by MOVPS [7] (12,060 evaluations), PMOGA [16] (25,050 evaluations), MODE [37] (15,030 evaluations), MOSFS[42] (25,050 evaluations) and MOFP [43] (25,050 evaluations) algorithms.

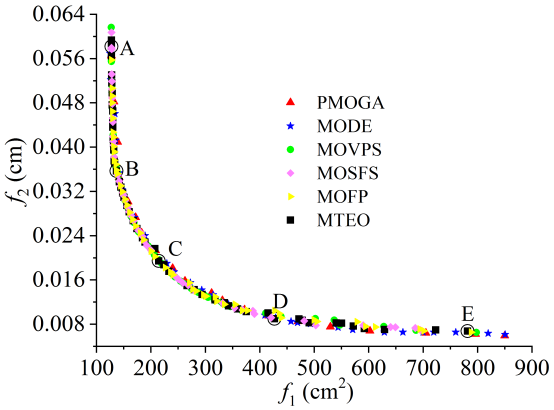

Figure 6. Pareto curve for the I-beam design (▲—PMOGA, ★—MODE, ●—MOVPS, ♦—MOSFS, ►—MOFP and ■—MTEO). A–E represent the points belonging to the optimal solution obtained by the proposed algorithm.

In this figure, it can be observed that the MTEO algorithm provides a good approximation of the Pareto curve when compared to the MOVPS, PMOGA, MODE, MOSFS and MOFP strategies. The main differences are attributed to the scattering quality of the proposed methodology in the extreme solutions found. Additionally, a reduction in the cross-sectional area of the I-beam (f_1) results in an increase in the maximum static displacement (f_2), and vice versa, highlighting the conflicting nature of the objectives. Regarding computational effort, assessed by the percentage minimizing the number of times the objective function is evaluated, the MTEO strategy achieved a substantial reduction of 52% and 20% compared to the PMODE (MOSFS, MOFP) and MODE algorithms, respectively. This demonstrates that the proposed algorithm not only reduces the number of objective function evaluations but also achieves solutions exhibiting both high convergence quality and diversity.

Table 3 presents some points corresponding to the optimal solution obtained by MTEO. The extreme points obtained by MTEO prioritize a single objective, allowing either a minimum deflection with an area of 781.5910 cm^2 (point E) or a minimum area with a deflection of 0.0581 cm (point A). The intermediate points show two design variables with common results (x_1 assuming its maximum value and x_3 assuming its minimum value). Points B and D correspond to more specialized solutions, minimizing f_1 and f_2, respectively, while point C represents a good compromise between the objectives, i.e., neither objective is prioritized in the minimization.

Table 3. Some points on the Pareto curve obtained by MTEO for the I-beam design problem. These points were selected because they represent favorable trade-offs in the optimal solution.

	A	**B**	**C**	**D**	**E**
x_1 (cm)	62.5089	80.0000	80.0000	80.0000	78.6132
x_2 (cm)	40.4884	37.0032	46.5806	50.0000	47.3172
x_3 (cm)	0.9000	0.9000	0.9000	0.9000	4.9364
x_4 (cm)	0.9000	0.9000	1.5590	3.6161	4.6426
f_1 (cm^2)	127.5172	136.9858	214.4328	427.1079	781.5910
f_2 (cm)	0.0581	0.0357	0.0194	0.0089	0.0067

6.2.2. MTEO parameters

Table 4 presents the influence of MTEO parameters on the area under the Pareto front of I-beam design problem. As observed in **Table 4**, the combinations of the considered parameters result in area values close to those computed using the MOVPS (7.8564), POGA (7.8943), and MODE (7.8887) strategies. This indicates that, regardless of the parameter values, the MTEO algorithm consistently converges to a close approximation of the Pareto curve, demonstrating the robustness of the proposed method.

Table 4. Influence of MTEO parameters on the area under the Pareto front of the I-beam design problem.

c_1	c_2	ρ	**Area**	c_1	c_2	ρ	**Area**
0.25	0.50	0.05	7.8834	0.50	0.25	0.05	7.8528
0.45	0.50	0.10	7.8656	0.50	0.45	0.10	7.8566
0.55	0.50	0.15	7.9523	0.50	0.55	0.15	7.8786
0.60	0.50	0.20	7.9381	0.50	0.60	0.20	7.8345
0.80	0.50	0.25	7.8656	0.50	0.80	0.25	7.8034
0.90	0.50	0.30	7.9234	0.50	0.90	0.30	7.9086

6.3. Welded beam design problem

This application considers the welded beam design, where the aim is to determine the dimensions of the weld and beam (x_1, x_2, x_3, and x_4) to minimize both the fabrication cost (Equation (26)) and the free end displacement of the beam (Equation (27)), as shown in **Figure 7**. This problem is constrained by limits on shear stress (τ), bending stress (σ), buckling load (P_c), end deflection (δ), as well as additional side constraints.

Mathematically, the mechanical design problem is formulated as follows [16]:

$$\min f_1 = 1.10471 x_1^2 x_2 + 0.04811 x_3 x_4 (L + x_2) \tag{26}$$

$$\min f_2 = \frac{4FL^3}{x_3^3 x_4 E} \tag{27}$$

$$\tau - \tau_{\max} \leq 0 \tag{28}$$

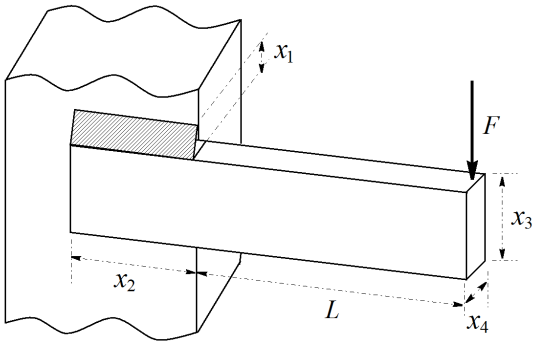

Figure 7. Schematic representation of a welded beam design.

Mathematically, the mechanical design problem is formulated as follows [16]:

$$\sigma - \sigma_{\max} \leq 0 \tag{29}$$

$$F - P_c \leq 0 \tag{30}$$

$$\frac{4FL^3}{x_3^3 x_4 E} - u_{\max} \leq 0 \tag{31}$$

$$x_1 - x_4 \leq 0 \tag{32}$$

where:

$$\tau = \sqrt{\tau_1^2 + \tau_2^2 + \frac{x_2 \tau_1 \tau_2}{\sqrt{0.25(x_2^2 + (x_1 + x_3)^2)}}} \tag{33}$$

$$\tau_1 = \frac{6000}{\sqrt{2} x_1 x_2} \tag{34}$$

$$\tau_2 = \frac{6000(14 + 0.5x_2)\sqrt{0.25(x_2^2 + (x_1 + x_3)^2)}}{2(0.707 x_1 x_2 (x_2^2/12 + 0.25(x_1 + x_3)^2))} \tag{35}$$

$$\sigma = \frac{504000}{x_3^2 x_4} \tag{36}$$

$$P_c = 64746.022(1 - 0.0282346 x_3) x_3 x_4^3 \tag{37}$$

This optimization problem presents the following lateral constraints [16]: 0.125 in $\leq x_1, x_4 \leq$ 5 in, 0.1 in $\leq x_2, x_3 \leq$ 10 in. It is important to mention that the coefficients (1.10471 and 0.04811) presented in Equation (26) are related to the material cost per unit of volume. Additionally, the following values are considered [16]: F = 6000 lb, $\tau_{\max}$ = 13,600 psi, $E = 30 \times 10^6$ psi, $\sigma_{\max}$ = 30,000 psi, $u_{\max}$ = 0.25 in, and L = 14 in.

To solve this test case, the following MTEO parameters are considered: N = 50, $NI_{\max}$ = 440, $c_1 = c_2$ = 0.5, and ρ = 0.3, i.e., 22,550 objective function evaluations. As previously stated, the choice of these parameters aims to reduce the computational cost while ensuring the quality of the Pareto curve.

6.3.1. Pareto curve

The Pareto curves obtained using each strategy are presented in **Figure 8**. As observed in this figure, there is a conflicting behavior between the objectives, along with a clear agreement between the results obtained by the proposed methodology and those from MOVPS, PMOGA, MODE, MOSFS and MOFP. Additionally, the figure shows a good scattering of the solutions along the Pareto curve. Concerning the number of objective function evaluations, the proposed methodology competes with the MOVPS [7] (24,100), PMOGA [16] (100,200), MODE [37] (25,050), MOSFS [42] (25,050), MOFP [43] (25,050) algorithms.

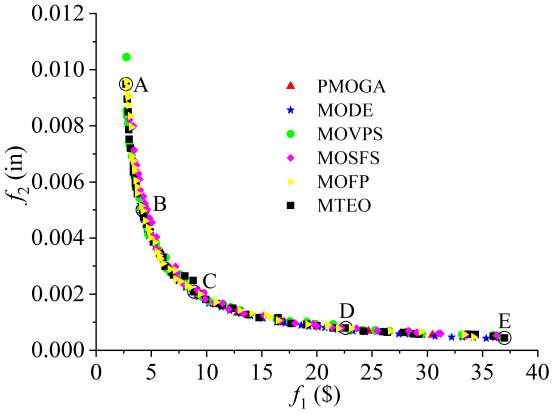

Figure 8. Pareto curve for the welded beam design (▲—PMOGA, ★—MODE, ●—MOVPS, ♦—MOSFS, ►—MOFP and ■—MTEO). A–E represent the points belonging to the optimal solution obtained by the proposed algorithm.

Regarding the percentage decrease with respect to the number of objective function evaluations, the MTEO strategy achieved reductions of 77%, 10%, and 7% compared to the PMODE, MODE (MOSFS and MOFP), and MOVPS algorithms, respectively. Therefore, the MTEO algorithm demonstrates a significant reduction in objective function evaluations relative to other evolutionary strategies.

In **Table 5**, selected points along the Pareto front considering the proposed methodology are presented. In this case, the beam width (x_3) approaches the maximum limit (10 in). In relation to other design variables, it appears that the increase in thickness (x_1 and x_4) accompanied by the reduction in beam length (x_2) leads to the minimization of beam deflection at the expense of increasing the price, and vice versa. The extreme points A and E prioritize, in particular, the lowest cost ($2.7037) and the lowest deflection (0.0004 in), respectively. Points B and D represent those that tend to favor one objective or the other, while point C seeks to balance the fulfillment of both objectives, resulting in a cost of $8.89165 at a deflection of 0.0021 in.

Table 5. Selected points along the Pareto front obtained by MTEO for the welded beam design problem. These points were selected because they represent favorable trade-offs in the optimal solution.

	A	B	C	D	E
x_1 (in)	0.2663	0.4623	0.8800	1.2239	1.7371
x_2 (in)	4.7725	2.5238	1.1874	1.2385	0.5760

Table 5. (*Continued*)

	A	B	C	D	E
x_3 (in)	9.4725	9.8059	9.8871	9.9282	10.0000
x_4 (in)	0.2723	0.46541	1.0901	2.8272	5.0000
f_1 (\$)	2.7037	4.224	8.8916	22.6279	36.9830
f_2 (in)	0.0094	0.0051	0.0021	0.0007	0.0004

6.3.2. MTEO parameters

Table 6 presents the area under the Pareto curve for different sets of parameters in the welded beam design problem. This table shows that the calculated area is close to those estimated using other strategies (MOVPS (0.0512), PMOGA (0.0532), and MODE (0.0515)). Additionally, the value of the obtained area indicates that the proposed methodology consistently converges to an accurate estimation of the Pareto front.

Table 6. Influence of MTEO parameters on the area under the Pareto front for the welded beam design case.

c_1	c_2	ρ	Area	c_1	c_2	ρ	Area
0.25	0.50	0.05	0.0501	0.50	0.25	0.05	0.0512
0.45	0.50	0.10	0.0511	0.50	0.45	0.10	0.0508
0.55	0.50	0.15	0.0522	0.50	0.55	0.15	0.0502
0.60	0.50	0.20	0.0523	0.50	0.60	0.20	0.0545
0.80	0.50	0.25	0.0533	0.50	0.80	0.25	0.0544
0.90	0.50	0.30	0.0511	0.50	0.90	0.30	0.0512

6.4. Robotic gripper design problem

The last case considers the design and structure of a robot gripper studied by other authors [48–55] and shown in **Figure 9**.

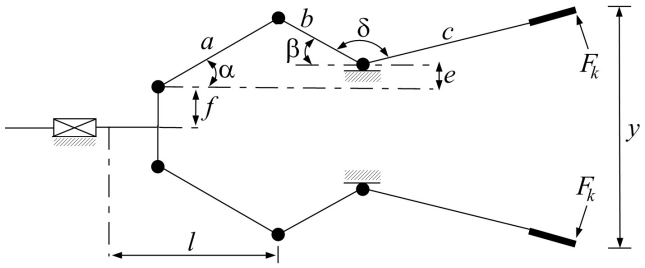

Figure 9. Schematic view of the gripper robot [54].

The aim is to determine the optimal link lengths (a, b, c, e, f, and l) of the gripper robot and the angle (δ) at the interface of elements b and c of the gripper to find the optimal solution that satisfies the given constraints and objective functions. The geometric constraints that couple the design variables is presented in **Figure 10**.

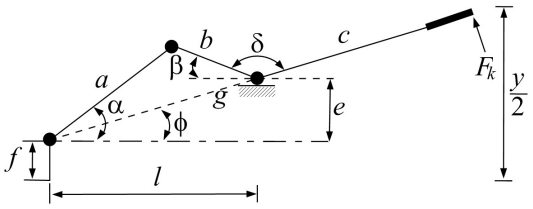

Figure 10. Geometric constraints of the gripper robot [54].

Mathematically, the following relations describe how these design variables are related:

$$g = \sqrt{(l-z)^2 + e^2} \tag{38}$$

$$b^2 = a^2 + g^2 - 2ag\cos(\alpha - \phi) \tag{39}$$

$$\alpha = \arccos\left(\frac{a^2 + g^2 - b^2}{2ag}\right) + \phi \tag{40}$$

$$a^2 = b^2 + g^2 - 2bg\cos(\beta + \phi) \tag{41}$$

$$\beta = \arccos\left(\frac{b^2 + g^2 - a^2}{2bg}\right) - \phi \tag{42}$$

$$\phi = \arctan\left(\frac{e}{l-z}\right) \tag{43}$$

The objectives are defined as:

i) Difference between the maximum and minimum griping forces (F_k) for the assumed range of gripper end displacement:

$$\min f_1(\mathbf{x}) = \max F_k(\mathbf{x}, z) - \min F_k(\mathbf{x}, z) \tag{44}$$

where:

$$F_k(\mathbf{x}, z) = \frac{Pb\sin(\alpha + \beta)}{2c\cos(\alpha)} \tag{45}$$

Let P represent the input force exerted from the left side to activate the gripper, and z denote a Cartesian coordinate. The vector $\mathbf{x} = (a, b, c, e, f, l, \delta)$ defines the system's design variables. Minimizing this objective ensures minimal variation in the gripping force throughout the entire operational range of the gripper [54].

ii) Force transmission ratio, i.e., the relation between the applied actuating force P and the resulting minimum gripping force at the tip of link c:

$$\min f_2(\mathbf{x}) = \frac{P}{\min F_k(\mathbf{x}, z)} \tag{46}$$

The minimization of this objective will ensure that the gripping force experienced at the tip of link c has the largest possible value [54].

As observed, each objective function depends on the design variables **x** and the

translation z (a parameter that takes a value from zero to $Z_{\max}$). Thus, for a given potential solution $\mathbf{x}$, it is necessary to determine both the maximum and minimum values of the gripping force $F_k(\mathbf{x}, z)$ for different possible values of z. For this purpose, these values are obtained using The standard Golden Section Search method [8,9].

Additionally, this mechanical design problem takes into account the following constraints [54]:

i) The dimension between ends of the gripper for the maximum displacement of the actuator should be less than the minimal dimension of the gripping object:

$$g_1(\mathbf{x}) \equiv Y_{\min} - y(\mathbf{x}, z) \geq 0 \tag{47}$$

where $y(x, z) = 2[e + f + c\sin(\alpha + \beta)]$ is the displacement of gripper ends and $Y_{\min}$ is the minimal dimension of the griping object, and $Z_{\max}$ denotes the maximal movement of the gripper actuator.

ii) The gap between the ends of the gripper referring to $Z_{\max}$ must be positive:

$$g_2(\mathbf{x}) \equiv y(\mathbf{x}, z) \geq 0 \tag{48}$$

ii) The distance between the gripping ends under zero actuator displacement (static condition) must exceed the largest dimension of the object being gripped.:

$$g_3(\mathbf{x}) \equiv y(\mathbf{x}, 0) - Y_{\max} \geq 0 \tag{49}$$

with $Y_{\max}$ being the largest dimension of the object to be gripped.

iv) The maximum displacement range of the gripper ends must be at least equal to the distance between the gripping ends when the actuator is at rest (static condition):

$$g_4(\mathbf{x}) \equiv Y_G - y(\mathbf{x}, 0) \geq 0 \tag{50}$$

with Y_G being the largest possible motion range of the gripper ends.

v) The following two constraints ensure the preservation of geometrical properties:

$$g_5(\mathbf{x}) \equiv (a + b)^2 - l^2 - e^2 \geq 0 \tag{51}$$

$$g_6(\mathbf{x}) \equiv (l - z_{\max})^2 + (a - e)^2 - b^2 \geq 0 \tag{52}$$

vi) Based on the gripper's geometry, the following constraint is derived:

$$g_7(\mathbf{x}) \equiv l - z_{\max} \geq 0 \tag{53}$$

vii) The minimum gripping force must be at least equal to the selected limiting gripping force:

$$g_8(\mathbf{x}) \equiv \min F_k(\mathbf{x}, z) - F_G \geq 0 \tag{54}$$

where F_G is the assumed minimal gripping force.

To design the robotic gripper using the MTEO algorithm, the following domains

are employed [54]: $10 \leq a \leq 250$ mm, $10 \leq b \leq 250$ mm, $100 \leq c \leq 300$ mm, $0 \leq e \leq 50$ mm, $10 \leq f \leq 250$ mm, $100 \leq l \leq 300$ mm, and $1.0 \leq \delta \leq 3.14$ (rad). Additionally, the following model parameters are considered: Y_{min} = 50 mm, Y_{max} = 100 mm, Y_G = 150 mm, z_{max} = 50 mm, P = 100 N, and F_G = 50 N.

The obtained results were compared using the following strategies: GA [52] (160,400 evaluations), NSGA^1 [54] (200,200 evaluations), SPEA-2 [55] (1,000,200 evaluations), NSGA^2 [55] (15,100 evaluations), MOVPS [7] (25,100 evaluations), and MTEO (N = 50, $NI_{\max}$ = 500, $c_1 = c_2$ = 0.5, and ρ = 0.3, i.e., 25,050 objective function evaluations).

6.4.1. Pareto curve

Figure 11 shows the Pareto curve obtained using all methods for optimizing the design of robotic grippers. In this figure, the conflicting nature of the objectives can be observed, irrespective of the optimization approach employed. Additionally, the Pareto curve produced by the MTEO algorithm closely matches that of MOVPS, with both methods surpassing all results found in the literature. Concerning the number of times the objective function was evaluated, the value needed by MTEO is comparable to that of MOVPS and smaller than the values required by the GA, NSGA^1, and SPEA-2 algorithms. However, it is larger than the value required by NSGA^2.

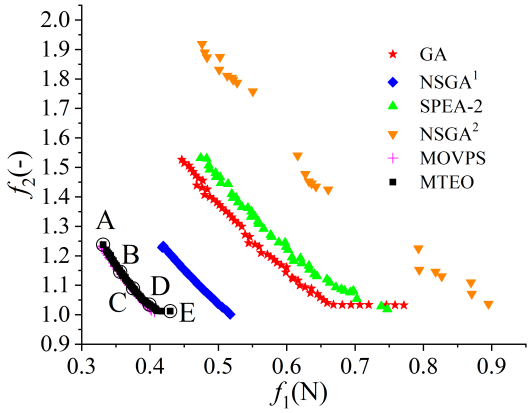

Figure 11. Pareto curve for the robotic gripper design problem (★—GA, ♦—NSGA^1, ▲—SPEA-2, ▼—NSGA^2, +—MOVPS and ■—MTEO). A–E represent the points belonging to the optimal solution obtained by the proposed algorithm.

Regarding the percentage decrease in the count of objective function calls, the MTEO strategy achieved decreases of 85%, 88%, and 98% compared to the GA, NSGA^1, and SPEA-2 algorithms, respectively. A similar number of evaluations was recorded when compared to the MOVPS algorithm. However, the MTEO algorithm required approximately 66% more evaluations than NSGA^2.

Table 7 presents selected points along the Pareto frontier acquired using the proposed methodology for the robotic gripper design problem. In these solutions, the parameters e and l tend toward their lower bounds, while parameters a, b, and c approach their upper bounds. The parameters f and δ assume intermediate values. Among the extreme solutions, points A and E respectively prioritize the minimum difference between the maximum and minimum gripping forces (0.3312 N) and the lowest force transmission ratio (1.0120). Points B and D represent trade-off solutions

that favor one objective over the other, whereas point C seeks to balance both objectives, resulting in a gripping force difference of 0.3752 N and a force transmission ratio of 1.0893.

Table 7. Some points along the Pareto frontier acquired using MTEO for the robotic gripper design problem. These points were chosen due to their representation of well-balanced trade-offs in the optimal solution space.

	A	**B**	**C**	**D**	**E**
a (mm)	249.8089	249.7975	249.7793	249.5774	249.4327
b (mm)	248.7482	248.8383	248.7906	248.6593	248.5579
c (mm)	300.0000	277.7093	264.0332	250.1488	244.3671
e (mm)	0.9298	0.8274	0.8554	0.7650	0.7116
f (mm)	60.0000	60.1743	60.2481	61.7152	62.4754
l (mm)	100.1138	100.1891	100.3902	102.9516	104.7952
δ (rad)	1.8000	1.8048	1.8095	1.8262	1.8350
f_1 (N)	0.3312	0.3563	0.3752	0.3992	0.4296
f_2 (-)	1.2376	1.1454	1.0893	1.0344	1.0120

6.4.2. MTEO parameters

Table 8 presents the influence of MTEO parameters on the area under the Pareto front for the robotic gripper design problem. This table shows that the calculated area is close to that estimated using MOVPS (0.0925), but significantly different from those obtained by other evolutionary strategies (see **Figure 11**). As all area values converged to a similar value, this indicates that the proposed methodology is robust in finding the approximation of the Pareto curve.

Table 8. Influence of MTEO parameters on the area under the Pareto trade-off curve for robotic gripper design.

c_1	c_2	ρ	**Area**	c_1	c_2	ρ	**Area**
0.25	0.50	0.05	0.0926	0.50	0.25	0.05	0.0923
0.45	0.50	0.10	0.0917	0.50	0.45	0.10	0.0921
0.55	0.50	0.15	0.0934	0.50	0.55	0.15	0.0962
0.60	0.50	0.20	0.0922	0.50	0.60	0.20	0.0922
0.80	0.50	0.25	0.0932	0.50	0.80	0.25	0.0936
0.90	0.50	0.30	0.0922	0.50	0.90	0.30	0.0921

7. Conclusions

In this study, the Multi-objective Thermal Exchange Optimization (MTEO) algorithm is introduced. This novel approach integrates the Thermal Exchange Optimization strategy with two well-established operators: Pareto dominance and crowding distance.

The proposed methodology was applied to a set of benchmark mathematical functions and mechanical engineering design problems of varying complexity. In terms of objective function evaluation efficiency, the MTEO algorithm achieved maximum reductions of 10.9%, 8.5%, and 19.9% for the ZDT_1, ZDT_2, and ZDT_3 problems,

respectively. For the I-beam design problem, MTEO achieved notable reductions of 52% and 20% compared to PMODE (MOSFS and MOFP) and MODE, respectively. In the Welded Beam design problem, the algorithm yielded reductions of 77%, 10%, and 7% relative to PMODE, MODE (MOSFS and MOFP), and MOVPS. In the case of the Robotic Gripper design problem, MTEO demonstrated a clear advantage, with reductions of 85%, 88%, and 98% compared to GA, NSGA[1], and SPEA-2, respectively. It showed a comparable performance to MOVPS (0.2% reduction), but required approximately 66% more evaluations than NSGA[2].

These results highlight the effectiveness of MTEO in approximating the Pareto front with high accuracy and maintaining good solution diversity. Across all test cases, the algorithm outperformed or matched the performance of existing evolutionary strategies, and the solutions obtained are consistent with the best results reported in the literature.

It is also noteworthy that, although the current study focuses on bi-objective problems, the MTEO algorithm can be readily extended to handle many-objective optimization scenarios. Like other population-based methods, MTEO requires the definition of a set of control parameters, which can be easily configured by the user.

Finally, as with most population-based optimization techniques, a key limitation of MTEO is the relatively high number of objective function evaluations. As a direction for future research, we intend to develop new operators to reduce computational cost, extend the methodology to handle multi-objective problems constrained by ordinary and partial differential equations—representing mass, energy, and momentum balances—and explore applications under uncertainty, aiming to optimize both reliability and robustness.

Author contributions: Conceptualization, FSL; methodology, FSL and FALM; software, FSL; validation, FSL and FALM; formal analysis, FSL and FALM; resources, FSL and FALM; writing—original draft preparation, FSL and FALM; writing—review and editing, FSL and FALM; project administration, FSL. All authors have read and agreed to the published version of the manuscript.

Funding: This research was funded by the Brazilian agency CNPq, grant number 309178/2023-1.

Conflict of interest: The authors declare no conflict of interest.

References

1. Pahl G, Beitz W, Feldhusen J, Grote KH. Engineering Design: A Systematic Approach, 3rd ed. Springer; 2007. p. 617.
2. Cross N. Design Thinking: Understanding How Designers Think and Work. Berg Publishers; 2011. p. 192.
3. Jin B, Xu X. Pre-owned Housing Price Index Forecasts Using Gaussian Process Pegressions. Journal of Modelling in Management. 2024; 19: 1927–1958. doi: 10.1108/JM2-12-2023-0315
4. Jin B, Xu X. Carbon Emission Allowance Price Forecasting for China Guangdong Carbon Emission Exchange via the Neural Network. Global Finance Review. 2024; 6: 3491–3507. doi: 10.18282/gfr.v6i1.3491
5. Jin B, Xu X. Machine Learning Predictions of Regional Steel Price Indices for East China. Ironmaking & Steelmaking.

2024; 2: 1–14. doi: 10.1177/03019233241254891
6. Jin B, Xu X. Wholesale Price Forecasts of Green Grams Using the Neural Network. Asian Journal of Economics and Banking. 2024; 3: 1–28. doi: 10.1108/AJEB-01-2024-0007
7. Andrade JC, Lobato FS, Neiro SMS, et al. A novel multi-objective optimization strategy based on vibrating particle system algorithm applied to chemical process design. Chemical Engineering Research and Design. 2024; 208: 161–183. doi :10.1016/j.cherd.2024.06.029
8. Vanderplaats GN. Numerical Optimization Techniques for Engineering Design, 3rd ed. Vanderplaats Research and Development; 2001. p. 449.
9. Edgar TF, Himmelblau DM. Optimization of Chemical Processes, 2nd ed. McGraw-Hill Science/Engineering/Math; 2001. p. 672.
10. Deb K. Multi-Objective Optimization using Evolutionary Algorithms, 1st ed. Wiley; 2001. p. 544.
11. Goldberg DE. Genetic Algorithms in Search, Optimization, and Machine Learning. Addison-Wesley; 1989.
12. Storn R, Price K. Differential evolution—a simple and efficient heuristic for global optimization over continuous spaces. Journal of Global Optimization. 1997; 11(4): 341–359. doi: 10.1023/A:1008202821328
13. Kennedy J, Eberhart R. Particle swarm optimization. In: Proceedings of the IEEE International Conference on Neural Networks; 27 November–1 December 1995; Perth, Australia. pp. 1942–1948.
14. Garcia VA, Finzi Neto RM, Lobato FS, Vieira, LGM. Reliability-based design of high-performance hydrocyclones: Multi-objective optimization, fabrication using 3D-printing and experimental analysis. Powder Technology. 2024; 435: 1–25. doi: 10.1016/j.powtec.2024.119427
15. Lobato FS, Alamy Filho JE, Libotte GB, Platt GM. Optimizing breast cancer treatment using hyperthermia: A single and multi-objective optimal control approach. Applied Mathematical Modelling. 2024; 127: 96–118. doi: 10.1016/j.apm.2023.11.022
16. Castro RE. Optimization of Structures with Multiobjectives by Pareto Genetic Algorithms (Portuguese). Departamento de Engenharia Civil—COPPE/UFRJ; 2001.
17. Lobato FS, Libotte GB, Platt GM. A novel multi-objective optimization method with local search scheme using shuffled complex evolution applied to mechanical engineering problems. Engineering Computations. 2022; 39: 2958–2989. doi: 10.1108/EC-07-2021-0381
18. Lobato FS, Lara-Molina FA, Libotte GB. A Comparative Study of Direct and Inverse Reliability Methods Applied to the Design of Robotic Manipulators. In: Kumar A, Bhandari AS, Ram M (editors). Reliability Assessment and Optimization of Complex Systems. Elsevier; 2024.
19. Lara-Molina FA, Dumur D. Robust multi-objective optimization of parallel manipulators. Meccanica. 2021; 56(11): 2843–2860. doi: 10.1007/s11012-021-01418-z
20. Kaveh A, Dadras A. A novel meta-heuristic optimization algorithm: Thermal exchange optimization. Advances in Engineering Software. 2017; 110: 69–84. doi: 10.1016/j.advengsoft.2017.03.014
21. Kaveh A, Dadras A. Structural damage identification using an enhanced thermal exchange optimization algorithm. Engineering Optimization. 2018; 50(3): 430–451. doi: 10.1080/0305215X.2017.1318872
22. Kaveh A, Dadras A, Bakhshpoori T. Improved thermal exchange optimization algorithm for optimal design of skeletal structures. Smart Structures and Systems. 2018; 21: 263–278. doi: 10.12989/sss.2018.21.3.263
23. Mahdad B, Djeblahi Z, Srairi K. Solving the energy management problems using thermal exchange optimization. Electrica. 2024; 24(2): 67–86. doi: 10.5152/electrica.2024.23045
24. Mohammed AM, Soufiene B. Thermal exchange optimization based control of a doubly fed induction generator in wind energy conversion systems. Indonesian Journal of Electrical Engineering and Computer Science. 2020; 20: 1–8. doi: 10.11591/ijeecs.v20.i3.pp1252-1260
25. Ragab M, Binaymin S. Intelligent energy-aware thermal exchange optimization with deep learning model for IoT-enabled smart healthcare. Journal of Healthcare Engineering. 2023; 2023: 1–13. doi: 10.1155/2023/3830857
26. Emadi M, Niaei M. Network intrusion detection using thermal exchange optimization and seagull optimization algorithm. Karafan Journal. 2023; 20(3): 509–529. doi: 10.48301/kssa.2023.389398.2481
27. Lagrari FE. Hybrid seagull optimization algorithm and thermal exchange optimization for optimal routing in VANET. Journal of Networking and Communication Systems. 2021; 4: 17–24. doi: 10.46253/jnacs.v4i3.a3
28. Kumar S, Jangir P, Tejani GG, Premkumar M. MOTEO: A novel physics-based multiobjective thermal exchange optimization algorithm to design truss structures. Knowledge-Based Systems. 2022; 242: 1–22. doi: 10.1016/j.knosys.2022.108422

29. Wolpert DH, Macready WG. No Free Lunch Theorems for Optimization. IEEE Transactions on Evolutionary Computation. 1997; 1: 67–82. doi: 10.1109/4235.585893
30. Alorf A. A Survey of Recently Developed Metaheuristics and Their Comparative Analysis. Engineering Applications of Artificial Intelligence. 2023; 117: 105622. doi: 10.1016/j.engappai.2022.105622.
31. Akan T, Anter AM, Etaner-Uyar AŞ, Oliva D. Engineering Applications of Modern Metaheuristics. Studies in Computational Intelligence. Springer International Publishing; 2023.
32. Sorensen K. Metaheuristics—the Metaphor Exposed. International Transactions in Operational Research. 2013; 22: 3–18. doi: 10.1111/itor.12001
33. Shirui S, Yang A, Chang C, et al. Improved Multiobjective Particle Swarm Optimization Integrating Mutation and Changing Inertia Weight Strategy for Optimal Design of the Extractive Single and Double Dividing Wall Column. Industrial & Engineering Chemistry Research. 2023; 62: 17923–17936. doi: 10.1021/acs.iecr.3c02427
34. Schaffer JD. Multiple objective optimization with vector evaluated genetic algorithms. In: Proceedings of the 1st International Conference on Genetic Algorithms; July 1985; Pittsburgh, PA, USA. pp. 93–100.
35. Pareto V. Cours D Economie Politique, volume I and II. University of Lausanne, 1896.
36. Deb K, Amrit P, Sameer A, Meyarivan TA. A fast and elitist multiobjective genetic algorithm: NSGA-II. IEEE Transations Evolutionary Computation. 2002; 6(2):182–197. doi: 10.1109/4235.996017
37. Lobato FS. Multi-objective Optimization for Engineering Systems Design (Portuguese) [PhD thesis]. Universidade Federal de Uberlândia; 2008.
38. Sadollah A, Eskandar H, Kim JH. Water cycle algorithm for solving constrained multi-objective optimization problems. Applied Soft Computing, 2015; 27: 279–298. doi: 10.1016/j.asoc.2014.10.042
39. Mirjalili S, Saremi S, Mirjalili SM, Coelho LS. Multi-objective grey wolf optimizer: A novel algorithm for multi-criterion optimization. Expert Systems with Applications. 2016; 47: 106–119. doi: 10.1016/j.eswa.2015.10.039
40. Mirjalili S, Jangir P, Saremi S. Multi-objective ant lion optimizer: A multi-objective optimization algorithm for solving engineering problems. Applied Intelligence. 2017; 46: 79–95. doi: 10.1007/s10489-016-0825-8
41. Heydarianas M, Fua'ad Rahmat M. Design optimization of electrostatic sensor electrodes via MOPSO. Measurement. 2020; 152: 1–25. doi: 10.1016/j.measurement.2019.107288
42. Lima JVCF, Lobato FS, Steffen Jr V. Solution of fractional optimal control problems by using orthogonal collocation and multi-objective optimization stochastic fractal search. Advances in Computational Intelligence. 2021; 1: 1–15. doi: 10.1007/s43674-021-00003-x
43. Silva CAX, Taketa E, Koroishi EH, Lara-Molina FA, Faria AW, Lobato FS. Determining the parameters of active modal control in a composite beam using multi-objective optimization flower pollination. Journal of Vibration Engineering & Technologies. 2020; 8: 307–317. doi: 10.1007/s42417-019-00133-0
44. Khodadadi N, Talatahari S, Dadras EA. MOTEO: A novel multi-objective thermal exchange optimization algorithm for engineering problems. Soft Computing. 2022; 26: 6659–6684. doi: 10.1007/s00500-022-07050-7
45. Zitzler E, Deb K, Thiele L. Comparison of Multiobjective Evolutionary Algorithms: Empirical Results. Evolutionary computation. 2000; 8: 1–15. doi: 10.1162/106365600568202
46. Carvalho R, Saldanha RR, Gomes BN, et al. A Multi-Objective Evolutionary Algorithm Based on Decomposition for Optimal Design of Yagi-Uda Antennas. IEEE Transactions on Magnetics. 2012; 48: 803–807. doi: 10.1109/TMAG.2011.2174348
47. Corder GW, Foreman DI. Nonparametric Statistics for Non-Statisticians: A Step-by-Step Approach, 1st ed. Wiley-Blackwell; 2009. p. 264.
48. Osyczka A. Evolutionary Algorithms for Single and Multicriteria Design Optimization, 1st ed . Heidelberg: Physica-Verlag; 2020.
49. Rao RV, Savsani VJ, Vakhaira DP. Teaching–learning-based optimization: A novel method for constrained mechanical design optimization problems. Computer Aided Design. 2011; 43(1): 303–315. doi: 10.1016/j.cad.2010.12.015
50. Cutkoski MR. On Grasp choice, grasp models, and the design of hands for manufacturing tasks. IEEE Transactions on Robotics. 1989; 5(3): 269–279. doi: 10.1109/70.34763
51. Li M, Qin QH, Zhang SW, Deng H. Optimal design for heavy forging robot grippers. Applied Mechanics and Materials. 2010; 44–47: 743–747. doi: 10.4028/www.scientific.net/AMM.44-47.743
52. Osyczka A, Krenich S. Some methods for multicriteria design optimization using evolutionary algorithms. Journal of Theoretical and Applied Mechanics. 2004; 42(3): 565–584.
53. Saravanan R, Ramabalan S, Ebenezer N, Dharmaraja, C. Evolutionary multi criteria design optimization of robot

grippers. Applied Soft Computing. 2009; 9(1): 159–172. doi: 10.1016/j.asoc.2008.04.001

54. Datta R, Deb K. Multi-Objective Design and Analysis of Robot Gripper Configurations Using an Evolutionary-Classical Approach. In: Proceedings of the 13th Annual Genetic and Evolutionary Computation Conference; 12–16 July 2011; Dublin, Ireland.
55. Avder A, Sahin I, Dorterler M. Multi-objective design optimization of the robot grippers with SPEA2. International Journal of Intelligent Systems and Applications in Engineering. 2019; 7(2): 83–87. doi: 10.18201/ijisae.2019252785